DOI 10.34658/jacs.2020.28.1.3-37

JOURNAL OF APPLIED
COMPUTER SCIENCE
Vol. 28 No. 1 (2020), pp. 7-37

Error Reduction for Static Localization

Barbara Morawska[1], Krzysztof Lichy[1], Piotr Koch[1], Jakub Niedźwiedzki[2], Marcin Leplawy[1], Piotr Lipiński[1],

[1]*Lodz University of Technology*
Institute of Information Technology
215 Wólczańska Str., 90-924 Łódź
234096@edu.p.lodz.pl,
krzysztof.lichy@p.lodz.pl,piotr.koch@dokt.p.lodz.pl,
mleplawy@gmail.com, piotr.lipinski@p.lodz.pl

[2] *Lodz University of Technology*
Institute of Machine Tools and Production Engineering
1/15 Stefanowskiego Str., 90-924 Łódź
jakub.niedzwiedzki@dokt.p.lodz.pl

Abstract. *This article describes methods for reducing the position measurement error of ultra-wideband localization system - DecaWave TREK1000. The static localization accuracy of this system can achieve 10cm. The localization algorithm introduced in this paper can improve it up to 1 centimeter. We could achieve such good accuracy, thanks to experiments that were carried out in various environmental conditions. This allowed us to identify the nature of the measurement error and design the correct set of filters.*
Keywords: *UWB, localization, Kalman filter.*

1. Overview of localization technologies

The position of objects in space can be determined using several technologies available on the market. Different features distinguish each of them: accuracy, susceptibility to disturbances or the surface that may be measured. Such diversity allows the system to be adapted to the expectations. The accuracy requirements will be different for a vessel sailing across the ocean and different for a doctor who locates the tumor inside the human body. In the first case, an error of a dozen of meters does not make a difference. In the second, millimeter precision is required because a larger error may have a negative impact on the patient's health or life. This work focuses on UWB positioning systems as they combine centimeter accuracy with low cost and relatively long-range. The comparison of available localization technologies is presented in Table 1.

Technology	**Accuracy**	**Range [m]**	**Principle of operation**	**Application**
Cameras	0.1 mm – dm	1 – 10	camera view angle	industry, robot navigation
Infrared	cm – m	1 – 5	thermal imaging measurements, navigation signal from transmitters	detection and tracking of living objects
Touch systems and systems based on the polar method	μm - m	3 – 2000	mechanical measurement, interferometry	industry, automotive

Sound	cm	2 – 10	distance calculation based on the time of travel	hospitals, object tracking
WLAN/WiFi	m	20 – 50	499.2	
RFID	dm – m	1 – 50	1081.6	
UWB	cm – m	1 – 50	distance calculated from travel time	robotics, automation
GNSS	10 m	global range	distance calculated from travel time	location services
Pseudo-satellites	cm – dm	10 – 1000	signal phase difference	GNSS support in places where its signal is poorly available or unavailable
Other radio frequencies (including Bluetooth)	m	10 – 1000	proximity measurement, signal strength measurement (RSSI), angle of arrival (AoA), angle of attack (AoD)	tracking people inside the space covered by the measurement
Inertial navigation	1%	110 – 100	Dead reconing	object tracking

Magnetic systems	mm – cm	1 – 20	magnetic field measurement	hospitals, mines

Table 1: Selected technologies of indoor location [1]

2. Localization using UWB

2.1. Characterisation of ultra-wideband waves

Ultra-wideband (UWB) technology is a method of radio communication over short distances which are relatively resistant to interference. Therefore it has found its application in indoor localization. Ultra-wideband waves are those whose bandwidth exceeds 500 MHz or 20% of the center of the carrier frequency [1]. To avoid interference with other radio signals, frequency ranges are limited. According to the European Communications Committee (ECC) directive Effective Isotropic Radiated Power (EIRP) of the signal generator antenna must not exceed -41.3 dBm / MHz [2], and the bands of used frequencies are limited depending on the region where they are used. For Europe, these values are from 6.0 GHz to 8.5 GHz (for comparison in the United States from 3.1 GHz to 10.6 GHz). The consequence of such restrictions is the possibility to use in Poland only some of the channels provided by producers of devices operating in UWB technology.

When studying the behavior of ultra-wideband waves it is worth considering how the signal is transmitted because it has a great importance in the context of its resistance to interference from other frequencies. Unlike GNSS or WLAN systems, UWB technology searches in vain for the signal carrier frequency. The term "frequency range" of the signal is used intentionally in this section. It is because the operation of UWB is based on the generation of very short pulses. With a short impulse and a large bandwidth, there are more advantages related directly to the location. It has an impact on the theoretical accuracy of the measuring device described by (1) [1].

UWB channel number	Middle frequency[MHz]	Frequency range	Bandwidth [MHz]
1	3494.4	3244.8 - 3744	499.2
2	3993.6	3774 – 4243.2	499.2
3	4492.8	4243.2 – 4742.4	499.2
4	3993.6	3328 – 4659.2	1331.2
5	6489.6	6240 – 6739.2	499.2
7	6489.6	5980.3 – 6998.9	1081.6

Table 2: 6 out of 16 channels compliant with the UWB IEEE802.15.4-2011 [2] standard supported by one of the most popular UWB modules, DW1000.

$$\Gamma\Gamma = \frac{v}{2b} \tag{1}$$

where v is the speed of the wave (approximately equal to the speed of light in a vacuum - 300,000,000 m /s), and b is the bandwidth (usually 500 MHz). Based on such assumptions, the theoretical accuracy of the device will be approximately 30 cm. As the bandwidth increases, the accuracy of the measurement will improve.

A short pulse of nano or even picosecond duration sent by the device and the legal restrictions imposed also affect the low power consumption of the UWB transmitter. The power consumption in such a device oscillates around 1 mW, which is approximately 1000 less than in WLAN technology (Figure 1), which can undoubtedly be considered as a remarkable feature [3].

The range of devices in the discussed technology is challenging to estimate because UWB waves are usually used inside buildings to penetrate through physical obstacles such as doors, windows or people. However, even disregarding these obstacles, and due to legal limitations in signal power, the maximum measurement distance will not exceed 100 m [1].

2.2. DecaWave TREK1000 measuring device

The DecaWave TREK1000 kit consists of 4 EVB1000 measurement plates (Figure 2), which have a removable antenna attached. From a technical point of view, this device is an STM32F105 ARM Cortex M3 microcontroller and a USB interface as well as an LCD. The element enabling work in UWB technology is

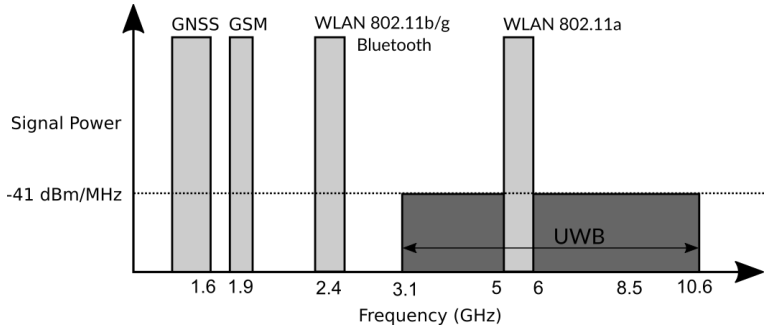

Figure 1: Comparison of popular technologies used for indoor locations in terms of used frequency and power spectral density. [1]

a particular DW1000 transceiver operating in the IEEE 802.15.4-2011 standard. Communication between the DW1000 and the microcontroller occurs through the serial interface of external devices (SPI - Serial Peripheral Interface) [4].

The device can be powered by both the USB port and an external power source with a voltage from 3.6V to 5.5V. The significant advantage of the board is the fact that due to the very low current requirements (the power supply must be able to supply 250 mA), it can be powered using popular and mobile power banks [5].

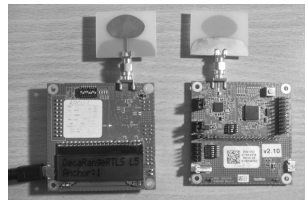

Figure 2: EVB1000 measuring plate with attached antenna. View from the side without the display - back (left) and with the display - front (right) [5]

The DW1000 integrated circuit placed on the board enables bi-directional transmission of measurement data at 110 kbps, 850 kbps, and 6.8 Mbps over six channels (Table 2). According to the manufacturer's datasheet, the accuracy of the provided device varies, depending on the measurement method, from ±10 cm to ±30 cm [5], which is far too optimistic according to the calculations provided in Chapter 2.1 from (1).

The maximum range of the DW1000 mainly depends on the transmission rate,

transmission frequency range and preamble length. The maximum measured distance varies from 60 meters at 6.8 Mbps to 250 meters at 110 kbps in a large open space. However, this coverage is unattainable due to legal restrictions. The indoor range is much smaller, especially when multiple obstacles interfere with the signal.

Another factor affecting the maximum operating distance of the UWB localization system is the channel and the associated center of the frequency range. The lower frequency, the greater range of the device. The bandwidth also affects the measuring range of the DW1000. Channels with a greater bandwidth (channels 4 and 7) will allow measurement over a greater distance than others. Unfortunately, using them will also consume more energy.

Although the bit rate and the used frequency have the greatest influence on the measuring range, the preamble length is also an essential factor. A preamble is a repetitive sequence of pulses with the pattern defined in the IEEE 802.15.4 standard and used to inform the receivers about the start of transmission. After hearing the preamble, the listening devices stop transmitting and prepare for receiving data. The problem would arise if the preamble did not arrive to the receiver on time due to the large distance between the transmitter and receiver, and it would start transmitting its signal. This is why at long distances, the preamble is very long to reach the receiver in time. The preamble lengths in the DW1000 device are adjusted to the baud rate (Table 3) [6].

Transmission speed	**Recommended preamble lengths**
6.8 Mbps	64 or 128 or 256
110 kbps	2048 or 4096

Table 3: Recommended preamble length depending on the baud rate [6]

The DW1000 IC is called the transceiver because it can exchange information with other systems that work the same way. However, it is worth mentioning that each board can work as a localized device (hereinafter called a tag) and as a locating device (called an anchor) mode. Therefore, whether a given device communicates with others as a tag or an anchor is not a hardware issue but a programmable one and it is determined just after powering the systems using DIP switches (Figure 3) [7].

Even though one switch is enough to determine the function of the device (whether it is a tag or an anchor), it is necessary to assign a unique identification

number to each of them. Determining such a number is carried out using three DIP switches. Since each of them can be arranged in two possible positions (top and bottom), theoretically, there are 8 identifiers for the tag and the anchor. However, hardware support was provided for up to 4 anchors. This restriction has not been imposed on localized devices. The reason for this is the communication method described during localization [7][8].

In addition to the functions of the device and its ID, the DIP switches are used to configure the measurement parameters. The function of each switch (see figure 3) is detailed in Table 4.

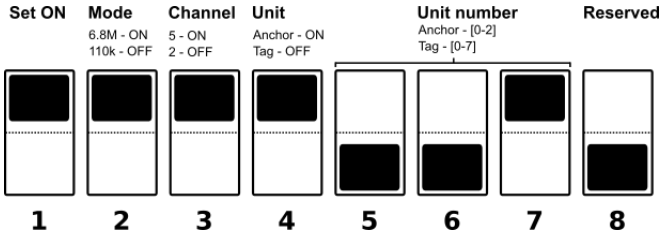

Figure 3: DIP switches with an indication of their purpose are located on each EVB1000 board [10]

The linearly polarized monopoly antenna is a critical element of each anchor and tag. It has been designed to obtain the best possible gain on UWB channels in the range from 3 GHz to 8 GHz. The antenna is best suited for use in a large open space. Therefore the condition for the correct work of the anchor is to place its antenna at least 15 cm from the nearest obstacle (especially walls). Simultaneously the antenna has omnidirectional characteristics, which enables precise measurement of the object's position throughout its range [11].

2.3. The method of position measurement with the DecaWave TREK1000

Measurement of the position of an object whose position is determined by anchors is based on sending timestamps between these devices. The difference in marker values between transmitting and receiving gives an opportunity to calculate how long it took for a wave to travel from one device to another. Knowing the time and the UWB wave velocity, it is possible to calculate the distance of the antenna and the tag (2).

$$s = v_{UVB} T_{prop} \tag{2}$$

Switch number	Top position	Bottom position	Comments
1	Starts the ARM processor or 128 or 256	The ARM processor does not start	If the user does not need the functionality offered by the microcontroller, but only access to the DW1000 chip, the switch can remain off.
2	The baud rate is set to 6.8 Mbps	The baud rate is set to 110 kbps	
3	The channel is set to 5 (center frequency - 6489.6 MHz, bandwidth - 500 MHz)	Channel is set to 2 (center frequency - 3993.6 MHz, bandwidth - 500 MHz)	The device also allows you to use other channels, but only for channel 2 and 5 has been properly calibrated.
4	The device is identified as an anchor	The device is identified as a tag	
5 **6** **7**	The baud rate is set to 6.8 Mbps	The baud rate is set to 110 kbps	Allows you to set the tag / anchor id as a binary number. For example, three anchors should be numbered: 000, 001, 010.
8	Enables the device response time to be changed remotely	Blocks the device's response time from remotely changing	By default, the response time of the device is 150 ms, but it can be changed using the PC application. If there is no such need, the switch should remain off.

Table 4: Description of switches for configuration of measurement parameters and EVB1000 board [9]

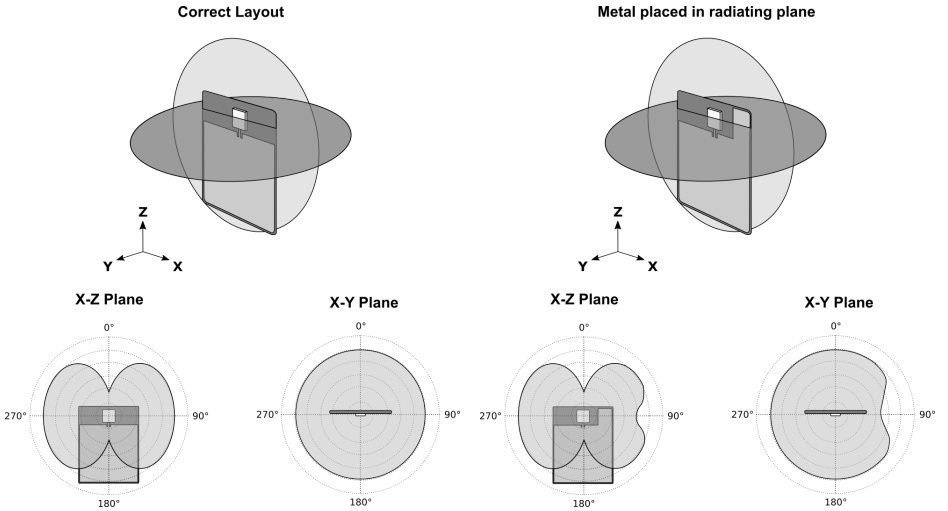

(a) Characteristics of a properly working, undisturbed antenna [11]

(b) Characteristics of the antenna disturbed by a nearby metal object [11]

Figure 4: Antenna characteristics

Theoretically speaking, the operation principle is therefore simple, but it is necessary to ensure that signals from multiple anchors and tags do not interfere with each other. Processing delays introduced by message encoding must also be taken into account. For this purpose, DecaWave uses an effective data exchange algorithm based on two-way communication between devices.

DecaWave TREK1000 uses so-called superframes. Each superframe has ten slots that can be used for data exchange between the tag and the anchors. As communication is duplex, superframes can support eight tags working with the same anchors. The remaining two slots are reserved for auto-positioning, i.e. the communication of anchors with each other without the participation of the tag [7].

The communication between devices within one slot starts with a tag that broadcasts a broadcast message "Poll" - to all four anchors simultaneously (even if only one is connected). Then it waits for responses from the anchors. After receiving a response, it ends the data exchange by transmitting a signal which terminates "Final" and enters sleep mode for the duration of the superframe [7].

At this point, it is worth mentioning that anchors are not equivalent. The most important function is performed by the anchor with identification number 000

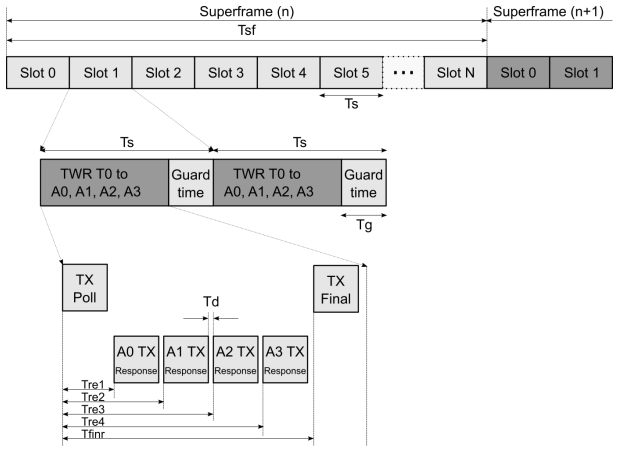

Figure 5: Diagram of communication between devices with the order in which the signals are transmitted [7]

(hereinafter A0). Without a correct connection between the tag and this anchor, the system will not work because only after receiving the answer from A0 the tag sends the Final message. In addition, the A0 anchor assigns slots to specific tags by giving them a fix related to their sleep time after the end of the transmission. This prevents the tags from interfering with each other. It also initiates communication between the anchors.

The other anchors, i.e. A1, A2, and A3 are optional. The functions A1 and A2 include communication with the tag and anchor A0 during auto-positioning. The anchor A3 does not communicate at all with any other device except the tag. It ignores all other signals.

Knowing all the above-mentioned details we are allowed to calculate the wave propagation time taking into account message processing times and their sequence. For the layout located in Figure 11, the time-of-flight determination will be consistent with (3).

$$\begin{aligned} \alpha T_{round1} &= 2T_{prop} + \beta T_{reply1} \\ \beta T_{round2} &= 2T_{prop} + \alpha T_{reply2} \\ 1 &= \frac{\alpha + \beta}{2} \end{aligned} \tag{3}$$

where α and β are the oscillator speeds (clocks) of devices A and B, the speed of which may vary slightly from each other but does not change during a single

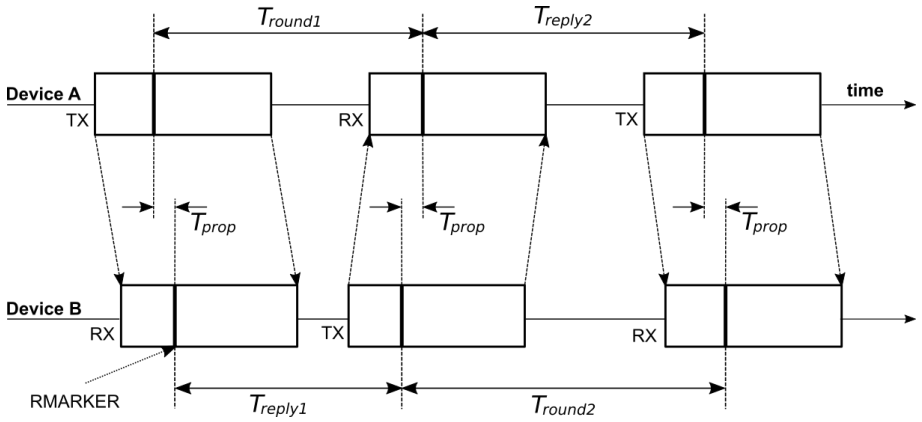

Figure 6: Scheme of message exchange between two devices [12]

slot. The remaining times, i.e. $T_{round(i)}$ and $T_{reply(i)}$ are respectively the time from sending the message to receiving the reply and the time elapsed between the receipt of the message and the sending of the reply [12].

As a result of transformation (3) it can be obtained that the propagation time is T_{prop} equal to:

$$T_{prop} = \frac{T_{round1}T_{round2} - T_{reply1}T_{reply2}}{T_{round1} + T_{round2} + T_{reply1} + T_{reply2}} \tag{4}$$

Substituting the time to (2) will allow you to calculate the distance from an anchor to tag [7] [12]. In a working system, the calculation of distances based on the example described above is shown in Figure 7.

2.4. Raw system data

Positioning data can be obtained by attaching a computer to an anchor or a tag via a USB port emulating a standard serial port. During the research, the computer that analyzed the results was always connected to the object being traced, i.e. to the tag. As a result of the positioning algorithm described in Chapter 2.3, the tag-anchor distance data is transmitted to the serial port, where it can be captured in the form of structured messages. An example of the message caught when the distance between the anchor and the tag equal to 0x5a2=1442mm and 0x500=1280mm is shown in Figure 8. When recording a message, the computer was pinned to a tag, and only one anchor was working - A0.

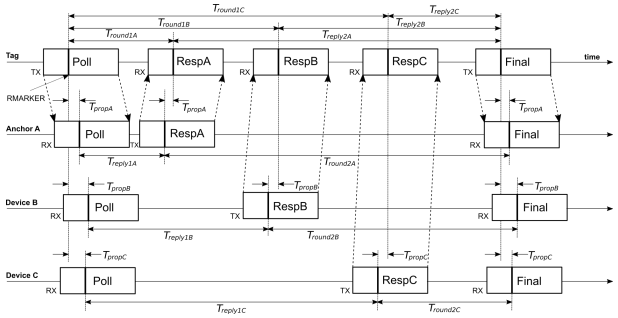

Figure 7: A method of synchronizing messages sent between devices that allows the calculation of the propagation time of the signal from each anchor to the tag [7]

```
mc 01 000005a2 00000000 00000000 00000000 0012 14 000023e1 t0:0

mr 01 000004da 00000000 00000000 00000000 0012 14 40524052 t0:0

mc 01 000005c8 00000000 00000000 00000000 0013 15 00002445 t0:0

mr 01 00000500 00000000 00000000 00000000 0013 15 40524052 t0:0
```

Figure 8: Messages intercepted by minicom when the computer is connected to the tag and only anchor A0 is running

3. Software

The raw data received from the DecaWave TREK1000 system can be further analyzed and interpreted. We used a laptop with the Ubuntu 18.04.3 LTS operating system and the Python programming language version 3.6.8. Additionally, the NumPy 1.17.0 package was used to perform more complex mathematical calculations, such as calculating the tag's position and reducing measurement error. The graphical presentation of the results and the configuration of the program parameters were performed using the MATLAB program by MathWorks.

4. Characteristics of the object location error

4.1. The sources of measurement error

Hypothetically speaking, a transmitter and a receiver located in a short distance from each other under ideal conditions and with precisely determined parameters will measure the distance without any error. If both devices do not move, each measurement will have the same value.

In practice, such a situation is physically impossible to implement. Currently manufactured electronic equipment has a finite accuracy in this case resulting from the stability and frequency of the oscillators. Also, the conditions under which such devices operate are far from being perfect. The equipment works in different rooms or outdoors, at different temperatures, and near other objects that may hinder its work.

For this reason, the accuracy of any measuring device is limited. The main sources of measurement error are:

- clock deviations on two or more measuring devices,
- changes in the signal level of a given device,
- signal multipath.

4.1.1. Errors caused by clock deviations

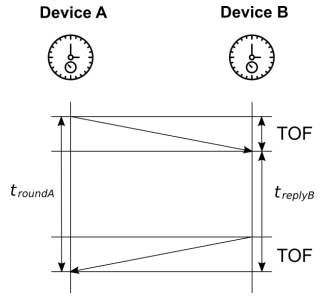

Figure 9: Diagram of communication between device A and device B. Each device has its own clock which has its own timing error independent of the other [13]

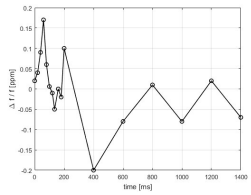

(a) Changes in the PPM value over time. The graph clearly shows the rapid changes in PPM in the first 400 ms of the oscillator operation, which is the result of its heating, as well as a natural physical phenomenon [13]

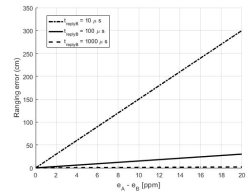

(b) Dependence of PPM on distance measurement error at different device response times. The graph shows that both the longer response time and the higher PPM value cause a rapid increase in the measurement error [13]

Figure 10: Characteristics of the PPM

Consider two DW1000 measuring devices communicating with each other (A and B - Figure 9), each of them has an independent crystal oscillator. The oscillators have time-varying errors, and in the literature, the difference between these values is called thermal stability - PPM (parts per million). This value allows determining the frequency range in which the clock runs. For example, a value of 20 PPM for an oscillator with a frequency of 38.4 MHz would mean that the actual clock is in the range of 38.399904 MHz (38.4 x 0.999980) to 38.400096 MHz (38.4 x 1.000020). These differences seem to be imperceptibly small, but assuming that there are 2.6 million seconds in a month, the clock error in this time will be over 60 seconds. A sample PPM graph overtime for a DecaWave system is shown in Figure 10(a).

Changes in PPM over time are difficult to predict and largely depend on the ambient temperature. Especially heating the quartz after it turns on affects their desynchronization.

Lack of synchronization of clocks and large fluctuations in PPM values between devices are the reasons why it is difficult to precisely determine the time of sending the message. Device A, not knowing that B is working at a different frequency will misinterpret its response. As a result, it will incorrectly calculate the time of flight. This error accumulates with the increase of B device response time (Figure 10(b)) [13].

4.1.2. Errors caused by changes in the signal level

The operation of location systems based on measuring the time of flight of a signal theoretically should not be related to the level of the received signal (RSL - Received Signal Level). In practice, it is difficult to eliminate this dependence completely. Although the signal strength in the DecaWave DW1000 measurement system does not have such an impact on the distance determination as in Bluetooth or WLAN technology, its influence is noticeable [13].

Figure 11 shows the exemplary instance (red line) where a change in RSL is not affected significantly by the actual waveform in any way (blue curve). Real measurements show that with a weak signal, the measured distances tend to be overstated, and with a strong signal, it tends to be understated. In the considered system, the optimal value at which no distortions occur is around -78 dBm.

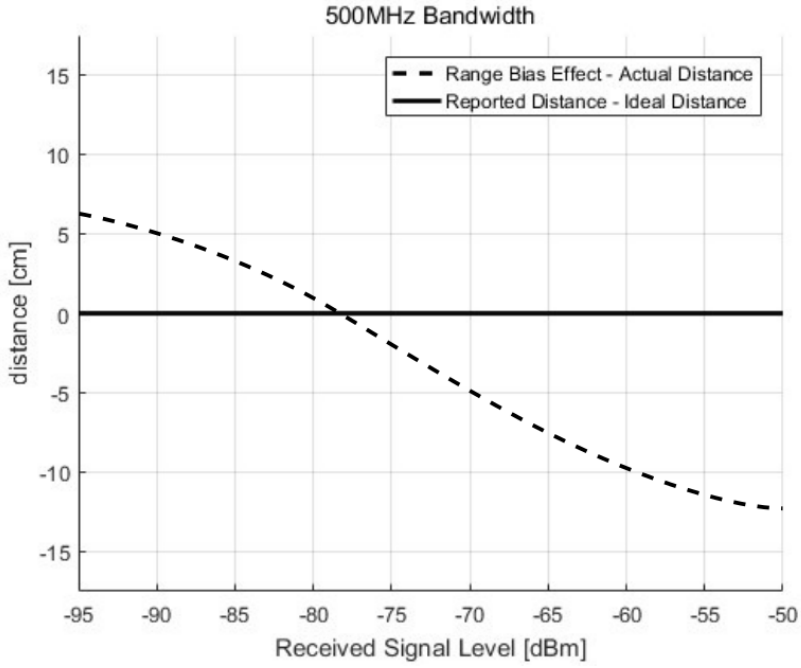

Figure 11: Influence of the received signal level on the accuracy of distance determination. The red line shows the model waveform in which the level of the received signal does not affect the measurement error, and the blue curve shows the real impact of these values on each other [13]

4.1.3. Signal multipath

In laboratory conditions, it is possible to build an ideal localization system where nothing prevents the signal from traveling between anchors and tags via the shortest possible route (called direct route). Such situation is presented in —. Such conditions are difficult to obtain in practice, as various types of obstacles appear on the signal path. As a result, the signal can travel from device A to device B by many routes, so the receiver acquires different distance values. In some simplification, this phenomenon is shown in Figure —, where the characteristic peaks indicate the registration of a data message. To select the correct impulse (direct route), it must be strong enough. Otherwise, the DW1000 will interpret it as a disturbance and take the reflected signal route as a correct value. The probability of making a mistake in such a situation is presented in Figure 12, which shows that the weaker direct route signal, the lower the probability the DW1000 will be able to select the correct message [14].

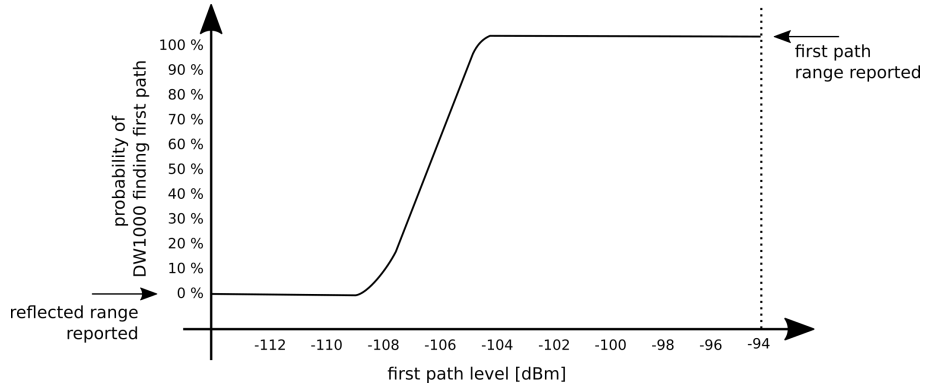

Figure 12: The graph of the probability that the DW1000 will find the first direct route depending on the signal level on this route [14]

The level of the signal that reaches the receiver depends on the distance between the receiver and the transmitter, as well as obstacles which the wave penetrates and is expressed in (5) [15]:

$$P_R[dBm] = P_T[dBm] + G[dB] - L[dB] - 20log_{10}(\frac{4\pi f_c(d_1 + d_2)}{c}) - L_{material}[dB] \quad (5)$$

P_T: radiated power

G: antenna gain (for DW1000 it is -41.3 dBm / MHz)

L: losses on the PCB, cable, connector, etc.

c: speed of light equal to 299792458 m / s

f_c: center frequency on a given channel in Hz

d_1, d_2: the distance from the transmitter to the obstacle and from the obstacle to the receiver (if there is no obstacle, the distance between the transmitter and the receiver should be substituted for the sum of the distance)

$L_{material}$: loss due to penetration through the given object (Table 5). The greater the attenuation, the weaker the signal

Material	**Attenuation at 4GHz**	**Comments**
Brick	-15dB	Thickness 89 mm
Concrete wall	-24dB	Thickness 102 mm
Concrete wall	-73dB	Thickness 306 mm
Plasterboard wall	0dB	Thickness 15 mm
Human body	-15dB to -30dB	Depending on the angle of incidence of the incoming signal and the body mass index.
Plywood	-1.5dB	Thickness 22 mm

Table 5: Attenuation of the signal by objects commonly found in buildings [15]

4.2. Error distribution depending on various environmental conditions

According to the analysis from Chapter 4.1, the equation (5) in particular, the measurement error increases in function of the distance between the transmitter

and the receiver. An experiment was carried out to check how these values actually change in relation to each other, and how the device settings influence them. We performed several distance measurements using DecaWave TREK1000 and LOMVUM LV 66U laser gauge. The laser gauge was considered as a reference, as its accuracy equals to ±1mm. Such measurements were performed several times for each distance value, ranging from 1 to almost 25 m.

(a) The conditions in which the tests were carried out were significantly different from typical laboratory conditions

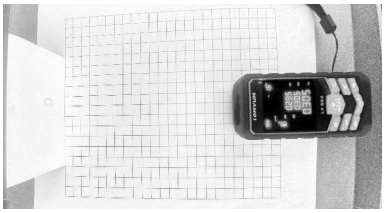

(b) Distance measurement with the LOMVUM gauge LV 66U

Figure 13: Research environment

The experiment was carried out in the open space to avoid reflections from the walls, as well as interference and attenuation of the signal caused by the presence of other objects and people.

During all tests, the data transmission speed was set to 6.8 Mbps and channel to 5. The resultant measurement error histograms are presented in figure 14. Each histogram was generated based on 10,000 measurements. The solid black line represents theoretical gaussian distribution corresponding to a given distance [16]. The measurement value is close to theoretical for low distance values and increases with the distance.

This is particularly noticeable in Figure 14(f) because the number of class ranges is much smaller than in other distances (35 vs 3), shifting the cluster of points to the left edge.

The histograms also show that the DW1000 system tends to underestimate results, i.e. in most cases, both the mean, median and mode values are below the reference distance by up to 2% (Table 6). This clearly affects the localization error determined using a triangulation algorithm. Simultaneously, gaussian distribution width is a very important parameter of the histogram, which determines the error characteristics (4.3) and constitutes a key parameter of the Kalman filter.

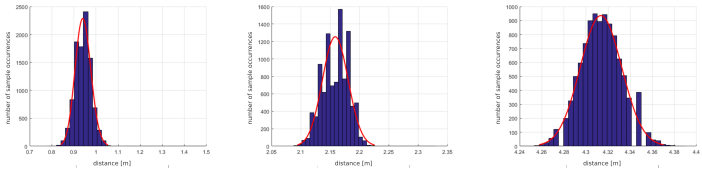

(a) Distance: 1,000 m, transmission speed: 6.8 Mbps

(b) Distance: 2,200 m, transmission speed: 6.8 Mbps.

(c) Distance: 4.350 m, transmission speed: 6.8 Mbps

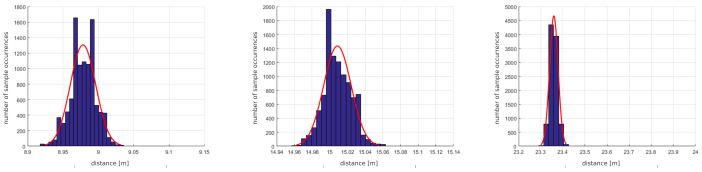

(d) Distance: 9.060m, Transmission Speed: 6.8 Mbps

(e) Distance: 14.990 m, transmission speed: 6.8 Mbps

(f) Distance: 23.590 m, transmission speed: 6.8 Mbps

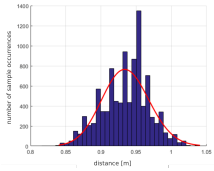

(g) Distance: 1.000m, Baud Rate: 110kbps, Average: 0.9356m, Standard Deviation: 0.0333.

Figure 14: Sample measurement session

Another experiment was carried out to understand the behavior of the DW1000 measurement error at different bit rates, i.e. 6.8 Mbps and 110 kbps. The experiment was performed at a distance of 1 meter from the anchor to the tag. The resulting histograms for the 6.8 Mbps and 110 kbps bit rates are illustrated in Figures 14(f) and 14(g). With slower data transmission, the obtained results have a much larger standard deviation. The full 10,000 measurements were also made in a much longer time. It is therefore not worth using the 110 kbps baud rate at short distances.

Reference distance [m]	Distance measured with the DecaWave DW1000 system [m]				
	arithmetic average	median	dominant	variance	standard deviation
1.000	0.9420	0.9460	0.9550	0.0013	0.0358
2.200	2.1589	2.1590	2.1640	0.0004810	0.0219
4.350	4.3136	4.3130	4.3080	0.0003519	0.0188
9.060	8.9782	8.9790	8.9790	0.0003247	0.0180
14.990	15.0087	15.0060	15.0060	0.0002421	0.0156
23.590	23.359	23.3570	23.3520	0.0003744	0.0194

Table 6: Characteristic values of sample distributions from histograms

A series of tests with one tag and one anchor made it possible to check how the measurement error behaves at different distances but did not guarantee that the errors would not interfere with each other with three anchors. In order to exclude this possibility, the system of 3 anchors and the tag was also tested to investigate the cross-correlation of measurements. What matters in the interpretation of cross-correlation charts is that these values should be small, which is the case of the DecaWave TREK1000 set.

The next aspect that was also examined was the mutual influence of successive measured samples on each other, called autocorrelation. As in the case of cross-correlation, the autocorrelation values should also be as small as possible, which is also in this case see (Figure 15(c)).

Our experiments showed that signal multipath (described in details in Chapter 4.1.3) strongly influences the localization results in the DecaWave TREK1000 set. Figure 15(d), shows the distance value distribution when multipath propagation between the anchor and the tag is possible. The red curve approximates the distribution of the samples to the distribution of the sum of two normal distributions. The histogram of such disturbed signal is clearly bimodal, which makes it very difficult to interpret correctly, as the mean, median, or dominant describe significant signal features only for unimodal distributions. Therefore, when reducing the measurement error, the filters should be applied to eliminate such cases.

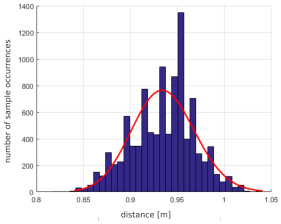

(a) Distance: 1.000m, Baud Rate: 110kbps, Average: 0.9356m, Standard Deviation: 0.0333.

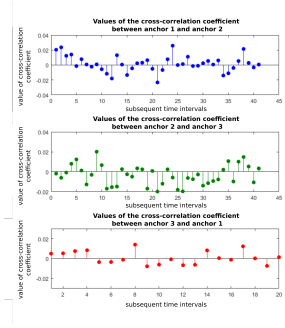

(b) The values of the cross-correlation coefficient between each pair of anchors

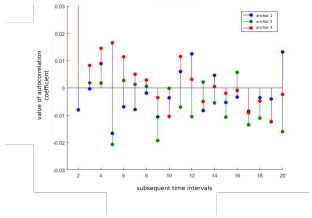

(c) Values of the autocorrelation coefficient of all anchors within 2 seconds

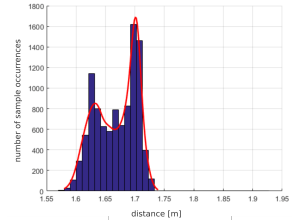

(d) Sample distribution disturbed by a human passing the direct route between the tag and the anchor

Figure 15: Experiment results

4.3. Determination of the error characteristic depending on the distance

The measurement error and variance changes with increasing distance between the tag and the anchor (see sec. 4.2). It has turned out that this kind of error cannot be easily corrected as the measurements error characteristics change significantly in function of tag location, see Figure 16. These characteristics not only depend on relative tag location but also depend on surrounding environment, which is illustrated in Figures 17 showing a measurement results in a large, open area.

Ultimately, the most truthful statement about the nature of the measurement error will be that its value varies with distance, but for each location where local-

ization is performed, the function will be different. For this reason, before starting the positioning process, the characteristics for a specific area should be determined.

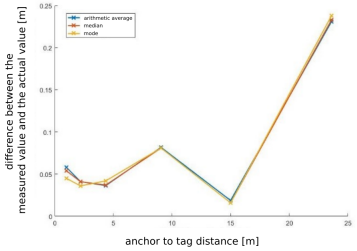

(a) The difference between the measured value and the actual value in relation to the distance of the tag from the anchor

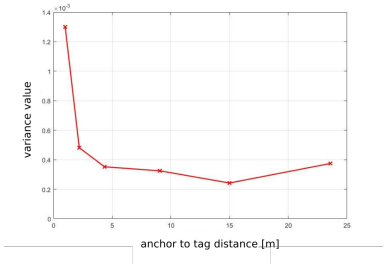

(b) The dependence of the variance value on the anchor distance from the tag

Figure 16: Short distance values

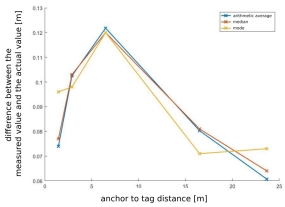

(a) The difference between the measured value and the actual value in relation to the distance of the tag from the anchor

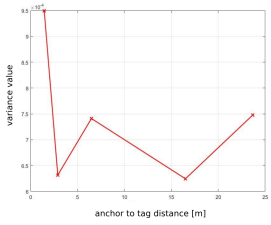

(b) The dependence of the variance value on the anchor distance from the tag

Figure 17: Long distance values

5. Error reduction during positioning

5.1. Raw data

The analysis described in previous sections analyzes the sources and characteristics of errors of UWB localization system. Here we measure the performance

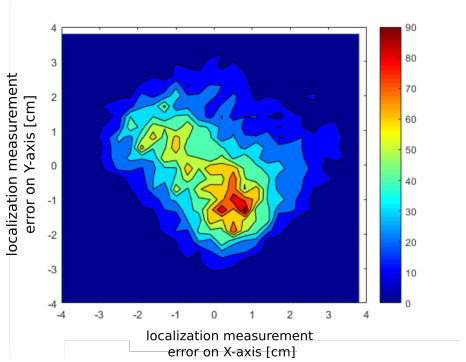

Figure 18: Distribution of sample positions in two-dimensional space when locating a stationary object without the use of filters

of the DecaWave system consisting of three anchors and one tag. The experiment was carried out at a short distance, where the anchors were 2-3 meters apart, and the tag was placed between the antennas.

Figure 18 shows the measurement error on the 2D plane. The graph is divided into 100 class intervals (10 in each axis) what gives us one for every 0.64 cm^2. We treat the difference between the reference position and the localization of histogram dominant as a measure of the error value. The center of the plot is snapped to the mean of all samples in both axes. Figure 18 shows that most measurements concentrate on average. The error distribution is within (± 3 cm) on each axis, but the OX axis results are more concentrated than on the OY axis. This is probably due to the environmental conditions and anchor localization.

The research aimed to compare the potential for the use of three different filters:

- median filter,
- the ARMA averaging filter,
- Kalman filter,

to reduce of the localization error of DecaWave 1000 localization system.

5.2. Median filter

The median filter is based on the concept of the median operator, which finds the middle value from the sorted array of a given length (called filter length). The OX axis values and the OY axis are filtered separately and then combined to get the new coordinate. As the system in question is a real-time system, this window significantly impacts the filter delay. The message with measurements arrives from the DecaWave device to the computer every 100 ms, so with a window of 3, the delay will be half of its length, i.e. 150 ms, while with a window of 20, it will be equal to 1 second. For this reason, the median filter does not perform well in such systems. However, this filter performs very well in short-term disturbances because it will be to ignore disturbed measurements.

The localization measurement errors for the median filter are shown in Figure 19. Each graph corresponds to the different median filter length. The increase of the window size reduces the measurement error in both dimensions, and with a window size of 19, it drops to (± 1 cm). Although the filter allows reducing the measurement error up to three times, it is not suitable for use in real-time systems, such as DecaWave TREK1000, due to the localization lag. The maximum number of samples in one class interval also increases with increasing the window size from 160 to 700 for the extreme window values tested (3 to 19), which is more than two-fold and almost eight-fold improvement over the unfiltered signal, respectively.

5.3. ARMA filter

The autoregressive-moving-average (ARMA) filter is a first-order infinite impulse response filter. In its general embodiment, an infinite impulse response (AR) filter is defined as follows:

$$Y(z) = H(z)Y(z) = \frac{\beta(1) + \beta(2)z^{-1} ... + \beta(n+1)z^{-n}}{\alpha(1) + \alpha(2)z^{-1} ... + \alpha(m+1)z^{-m}} \tag{6}$$

where $\beta(i)$ and $\alpha(i)$ are the filter coefficients, n and m are the filter order. If n it is greater than zero, then the suffix moving-average (MA) can be added to the filter and hence the name ARMA.

Looking for the desired filter properties (low-pass, with gain 1), we decided to simplify (6) to the form:

$$Y(z) = \frac{\beta}{1 - \alpha z^{-1}} X(z) \tag{7}$$

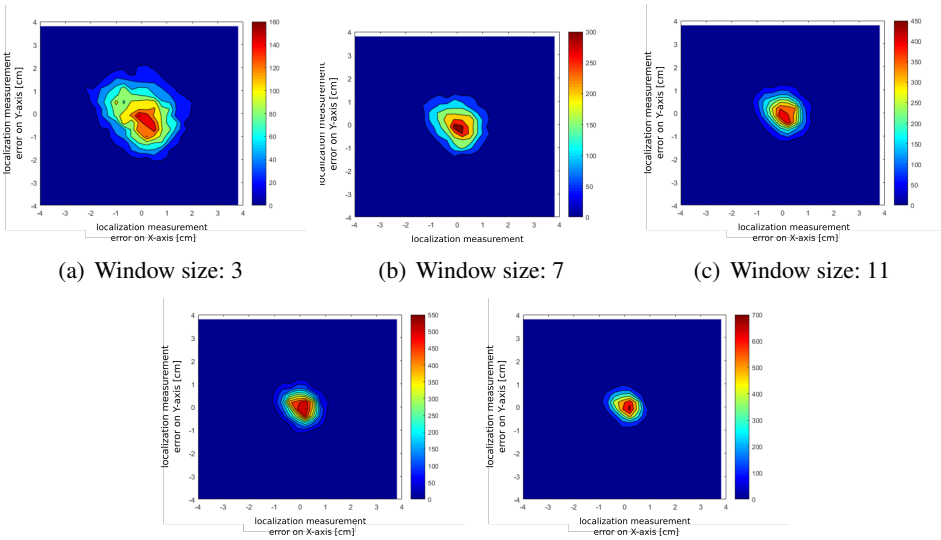

(a) Window size: 3 (b) Window size: 7 (c) Window size: 11

(d) Window size: 15 (e) Window size: 19

Figure 19: Median filter

where $\beta = 1 - \alpha$

The filter effect can be seen in Figure 20. It is easy to notice that the measurement error decreases with increasing the α coefficient. With the coefficient α = 0.95, it is already (± 1 cm). It is also worth mentioning that, unlike the median filter, there is no lag in this case (see: (7)). As the α coefficient increases, the maximum number of samples in the class range increases. In the case of α = 0.5, it is 180, which is about two times more than in the signal without filtration, but for α = 0.95, this value increases to 1800 measurements per interval, resulting in a 20 fold improvement.

Therefore, it can be said that despite the simplicity of the filter, it performs well and can be used to reduce the measurement error of a stationary object. The disadvantage of the algorithm is that if the tag started to move, increasing the α coefficient could lead to its sudden movements being ignored, because they would be treated as a measurement error and eliminated.

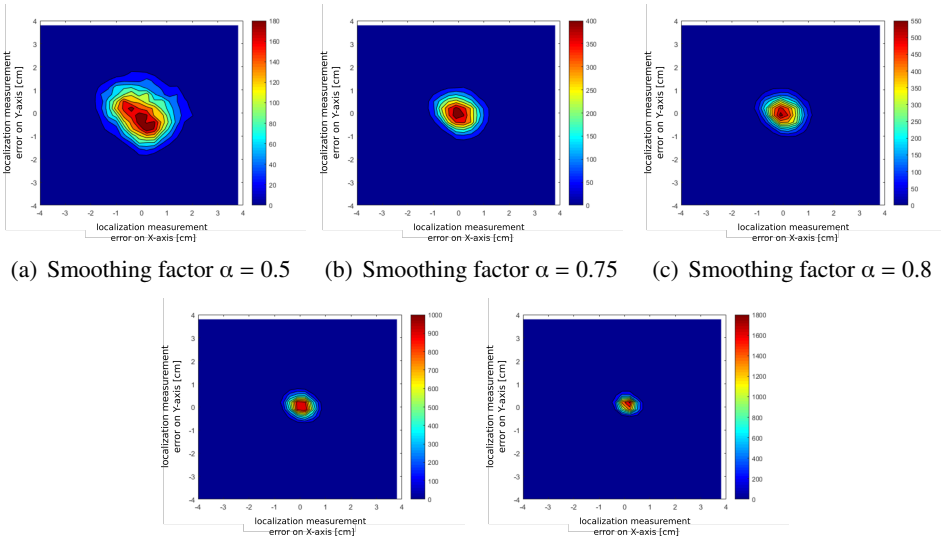

(a) Smoothing factor $\alpha = 0.5$ (b) Smoothing factor $\alpha = 0.75$ (c) Smoothing factor $\alpha = 0.8$

(d) Smoothing factor $\alpha = 0.9$ (e) Smoothing factor $\alpha = 0.95$

Figure 20: ARMA filter

5.4. Kalman filter

The Kalman filter is one of the best-known algorithms for recursive vector state determination with the smallest possible error for a linear model describing a discrete dynamical system based on the output measurements and the input of this system. It is most efficient when the error has a Gaussian distribution [17].

5.4.1. Application of the Kalman filter to object localization

The result of the localization signal filtration using Kalman filter is shown in Figure 21. The filter managed to reduce the position error on the OX and OY axes to (± 0.5 cm), that is, to obtain a value six times lower on each axis in relation to for measurements without the use of a filter (in Figure 18 this value was ± 3 cm). Taking into account the area of occurrence of the samples, it is about 36 times smaller. The largest number of measurements in the class range was as high as 5500, which means that more than half of the entire measurement session coordinates were located in almost the same place. The Kalman filter has no delay, but it does not react immediately to sudden changes (inertia).

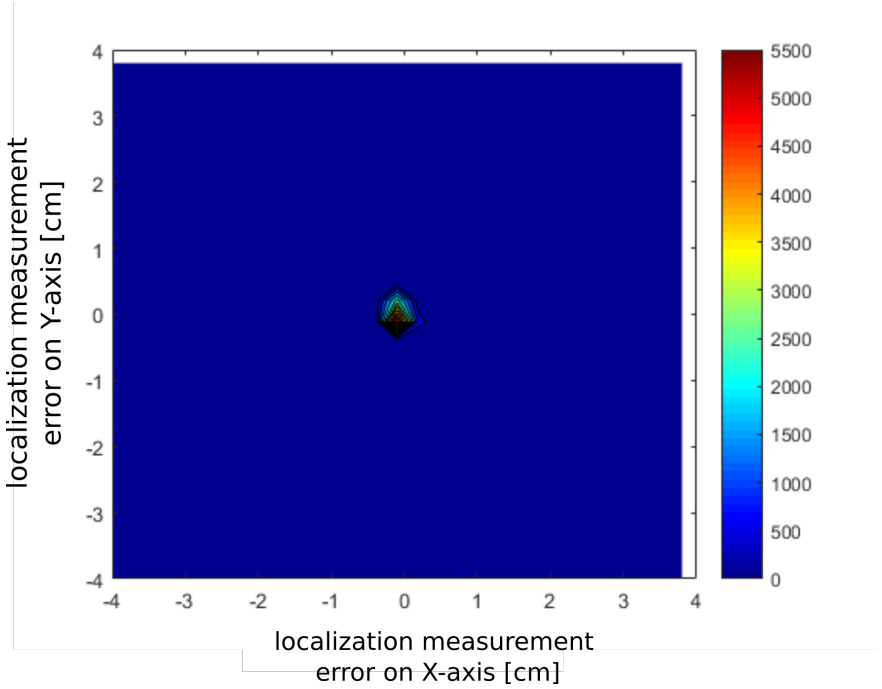

Figure 21: Distribution of sample positions in two-dimensional space at the location of a stationary object after using the Kalman filter

The experiment has shown that the Kalman filter is ideally suited for reducing the measurement error with UWB systems, enabling extremely precise localization that would not be possible without its use.

5.5. Results of analysis

Table 7 compares the filters used in terms of:

- position measurement error in the OX and OY axes - the highest which was achieved,
- filter delays - including those resulting from delayed response to abrupt changes,
- the maximum number of samples that appeared in the class range of the histogram (per 10,000).

Filter name	Position measurement error achieved [cm]	Delay	Maximum number of samples in the class range (per 10,000)
No filter	±3	0	90
Median filter	±1	Variable, $100\frac{k}{2}$ k - window size	700
ARMA filter	±1	0	1800
Kalman filter	±0.5	0	5500

Table 7: Summary of the best results that were achieved with each of the filters used

6. Conclusions

In this article, we have tested the localization accuracy of DecaWave 1000. We also applied the following three filters: median, ARMA, and Kalman filter to improve it. Particular emphasis was placed on the fact that the experiments were carried out in an environment similar to how the devices of this type actually work. This contrasts with most scientific articles written on the subject, based on research carried out in isolated laboratories and at short distances.

We also described the characteristics of the localization error system and analyzed it. We conducted the same experiments in different environments, which allowed us to draw the conclusion that the characteristics of the error strongly depends on the surrounding environment. The research has also shown that due to the transmission speed at distances below 25 meters, 6.8 Mbps transmission speed performs much better at 110 kbps.

An important observation was that the attenuation caused by obstacles strongly deteriorates the localization accuracy. We also demonstrated that the median filter can effectively neutralize short time localization disturbances.

We tested three types of filters: the median filter, the ARMA averaging filter and the Kalman filter. The best results were obtained for the Kalman filter. The second best filter was the ARMA averaging filter, which despite of a greater measurement error (± 1 cm), had no delay, and almost 20% of all measurements were in one class range. The median filter was the worst one. The main flaw of the median filter was the localization delay increasing with the location accuracy improvement. Despite of the obtained precision, almost identical to the ARMA filter,

the maximum number of samples in the class range did not exceed 10%.

The developed research results offer great potential for continuation, especially in dynamic localization, application of different filters, and artificial intelligence.

References

[1] Mautz, R., *Indoor positioning technologies, Habilitation Thesis submitted to ETH Zurich Application for Venia Legendi in Positioning and Engineering Geodesy*, Ph.D. thesis, ETH Zurich, 2012.

[2] Electronic Communications Committee, *The harmonised use, exemption from individual licensing and free circulation of devices using Ultra-Wideband (UWB) technology in bands below 10.6 GHz*, ECC Decision (06) 04, 2019.

[3] Haraz, O., *Why do we need Ultra-wideband?* https://www.vlsiegypt.com/home/?p=518, (Accessed: 23.11.2019).

[4] DecaWave, *Overview of EVB1000 Evaluation Board*, 2013.

[5] DecaWave, *TREK1000 User Manual*, 2016.

[6] DecaWave, *DW1000 User Manual*, 2017.

[7] DecaWave, *Range RTLS ARM Source Code – Understanding and Using the DecaRange RTLS ARM Source Code*, 2015.

[8] DecaWave, *TREK1000 Expansion Options Instructions*, 2016.

[9] DecaWave, *EVK1000 User Manual*, 2016.

[10] DecaWave, *Two-Way-Ranging (TWR) RTLS IC Evaluation Kit*, 2016.

[11] DecaWave, *APH001 Application Note. DW1000 Hardware Design Guide*, 2018.

[12] arnaud (Bitcraze forums), *DWM 1000 DS-TWR calculate distance method*, https://forum.bitcraze.io/viewtopic.php?t=1944#p9959, (Accessed: 23.11.2019).

[13] Decawave, *APS011 Application Note. Sources of Error in DW1000 Based Two-Way Ranging (TWR) Schemes*, 2014.

[14] Decawave, *APS006 Part 2 Application Note. Non Line of Sight Operation and Optimization to Improve Performance in DW1000 Based Systems*, 2014.

[15] Decawave, *APS006 Application Note. Channel Effects on Communications Range and Time Stamp Accuracy in DW1000 Based Systems*, 2014.

[16] Risset, T., Goursaud, C., Brun, X., Marquet, K., and Meyer, F., *UWB Ranging for Rapid Movements*, In: 2018 International Conference on Indoor Positioning and Indoor Navigation (IPIN), 2018, pp. 1–8.

[17] Saho, K., *Kalman Filter for Moving Object Tracking: Performance Analysis and Filter Design*, In: Kalman Filters, edited by G. L. O. Serra, chap. 12, IntechOpen, Rijeka, 2018.